Supplementary Materials: Biological and Physical Effects of Brine Discharge from Carlsbad Desalination Plant and Implications to Future Desalination Plant Constructions

Karen Lykkebo Petersen [1,2,*], Nadine Heck [3,4], Borja G. Reguero [3,4], Donald Potts [3,5], Armen Hovagimian [6] and Adina Paytan [3]

[1] Department of Earth and Planetary Sciences, University of California, Santa Cruz, 1156 High Street, Santa Cruz, CA 95064, USA
[2] Department of Ecology, Environment and Plant Science, Stockholm University, Svante Arrhenius väg 20A, 114 18 Stockholm, Sweden
[3] Institute of Marine Sciences, University of California, Santa Cruz, 1156 High St., Santa Cruz, CA 95064, USA; nheck@ucsc.edu (N.H.); borja_reguero@tnc.org (B.G.R.); potts@ucsc.edu (D.P.); apaytan@ucsc.edu (A.P.)
[4] The Nature Conservancy, 115 McAllister Way, Santa Cruz, CA, 95060, USA
[5] Department of Ecology and Evolutionary Biology, University of California, Santa Cruz, 130 McAllister Way, Santa Cruz, CA 95060, USA
[6] Cowell College, University of California, Santa Cruz, 1156 High Street, Santa Cruz, CA 95064, USA; ahovagim@ucsc.edu
* Correspondence: lykkebo.petersen@su.se

Wave Model

In coastal zones and estuaries, both temporal and spatial variations in salinity are controlled by changes in circulation, waves, tides, precipitation, evaporation, and freshwater inflows. Such changes in salinity can have major effects on water density and water column stratification, which can modify circulation patterns [1]. The salinity field can be calculated based on the salinity conservation equation (Eq S1), which depends on the flow of water in the coast.

$$\frac{\partial(Sd)}{\partial t}+\frac{\partial Sq_x}{\partial x}+\frac{\partial Sq_y}{\partial y}=\frac{\partial}{\partial x}\left[K_x d\frac{\partial S}{\partial x}\right]+\frac{\partial}{\partial y}\left[K_y d\frac{\partial S}{\partial y}\right]+(P-E)S \quad \text{(S1)}$$

where S is depth-averaged salinity; d is total water depth, q_x and q_y are flow per unit width in the x- and y-axis direction, respectively; K_x and K_y are diffusion coefficients of salt in the corresponding x- and y-axis direction, and P and E are precipitation and evaporation in m/year, respectively.

When exchange with the open sea is restricted within an inlet, tidal range may be the primary indicator of vertical mixing conditions. However, in open coastal waters, wave action is one of the main drivers of water circulation along the shore [1]. For Carlsbad, we focus on mixing in an open coastline with sufficient depth to ignore tidal and other effects, so that mixing is controlled by wave dynamics.

To study the mixing potential of wave action, patterns of wave energy and orbital velocity are calculated for the mean conditions for each season and averaged for the year. We used wave model data for the California continental shelf that provides information on wave heights, periods and orbital velocities at high resolution for the whole Californian coast including mean and extreme (top 5%) wave parameters for each season [1,2]. A 15 SWAN curvilinear grids were used to simulate wind-wave growth and propagation across the inner portion of the California continental shelf [2]. All grids had an average cross- and along-shore resolution of 30 to 50 m and 60 to 100 m, respectively, in shallow inshore regions. To enable accurate wave refraction and shoaling, model grid cells were smaller in the cross-shore direction, in shallow water, and around complex bathymetry.

As an indicator of water flow, we used the Wave Energy Density (i.e., the total energy per wave per unit width), which is also related to longshore currents, and is calculated as:

$$E=K\acute{E}+P\acute{E}=\frac{1}{8}\rho g H^2 \quad \text{(S2)}$$

$$E_L=\frac{1}{8}\rho g H^2 L \quad \text{(S3)}$$

As an indicator of annual mixing potential, E is calculated by averaging the mean conditions for each season. Because the North Pacific Ocean can generate extremely large surface waves and they can vary strongly between seasons and years [3,4], wave energy, in particular, is highly variable as a result of winter and summer storms and variation is also associated with inter-annual climate patterns like El-Nino. Therefore, we also map these seasonal variations that can be a key source of variability of mixing conditions.

In shallow water, the orbital motions of water particles induced by surface waves extend down to the seabed. Because resulting wave-induced orbital velocities near the seabed are considered to be representative measures of how waves influence the sea floor, they are a focus of this study [1]. The orbital velocity is used as an indicator of mixing potential at the seabed; mean seasonal values were obtained from Erikson et al (2014) [2] for each season and then averaged annually, similar to the wave energy density.

Water Chemical Properties

Table 1. Mean concentrations (with standard deviation in parenthesis) of Chl *a*, nutrients (NO_{3^-}, PO_4, SiO), and dissolved organic carbon (DOC), and $\delta^{13}C$ of particulate matter and C/N molar ratio of particulate matter from each sampling trip. Data separated into control and within the plume impact areas of the field site, and into bottom and surface water.

Sampling Trip	Area	Water Level	Chl *a* (μg L^{-1})	NO_3 (μM L^{-1})	PO_4 (μM L^{-1})	SiO (μM L^{-1})	DOC (μM)	$\delta^{13}C$ (‰)	C:N
December 2014	Control	Surface	1.33 (0.26)	0.94 (0.34)	0.68 (0.23)	2.68 (0.81)	146.4 (32.3)	NA	NA
		Bottom	1.27 (0.23)	2.55 (1.51)	0.67 (0.2)	4.44 (1.79)	124.1 (19.2)	NA	NA
	Plume	Surface	1.00 (0.13)	2.15 (2.5)	0.44 (0.21)	2.46 (0.21)	151.8 (NA)	NA	NA
		Bottom	1.05 (0.21)	1.02 (0.42)	0.41 (0.06)	2.53 (0.23)	95.4 (NA)	NA	NA
September 2015	Control	Surface	0.98 (0.19)	1.17 (1.38)	0.31 (0.08)	0.14 (1.64)	546.0 (572.9)	−22.8 (1.4)	6.8 (2.3)
		Bottom	0.86 (0.42)	0.79 (0.94)	0.44 (0.59)	0.11 (1.2)	241.1 (242.8)	NA	NA
	Plume	Surface	0.83 (0.35)	0.56 (0.24)	0.29 (0.05)	-0.29 (1.36)	515.6 (665.9)	−22.5 (5.3)	5.3 (1.1)
		Bottom	0.54 (0.25)	0.78 (0.75)	0.40 (0.41)	1.31 (2.94)	648.8 (796.3)	NA	NA
May 2016	Control	Surface	2.07 (0.81)	3.40 (2.41)	0.40 (0.15)	5.27 (1.97)	423.8 (529.1)	−22.3 (8.1)	8.1 (2.6)
		Bottom	2.28 (0.35)	1.27 (1.19)	0.28 (0.11)	4.20 (1.5)	901.3 (1107.3)	NA	NA
	Plume	Surface	1.24 (0.41)	2.51 (4.01)	0.38 (0.23)	6.11 (3.08)	529.0 (774.5)	−22.9 (6.9)	6.9 (0.7)
		Bottom	1.23 (0.24)	0.58 (0.64)	0.76 (1.76)	5.99 (4.72)	1086.9 (NA)	NA	NA
November 2016	Control	Surface	1.53 (0.44)	1.65 (1.65)	0.64 (0.22)	3.92 (3.03)	231.4 (460.3)	−22.3 (0.4)	7.2 (0.5)
		Bottom	1.54 (0.53)	0.86 (1.4)	0.63 (0.17)	5.62 (5.96)	58.0 (27.2)	NA	NA
	Plume	Surface	1.56 (0.37)	0.64 (0.52)	0.71 (0.05)	3.22 (1.39)	147.6 (169.4)	−22.6 (1.9)	7.4 (1.3)
		Bottom	1.33 (0.55)	0.39 (0.54)	0.68 (0.06)	2.88 (0.64)	206.7 (347.7)	NA	NA

Benthic Macrofauna

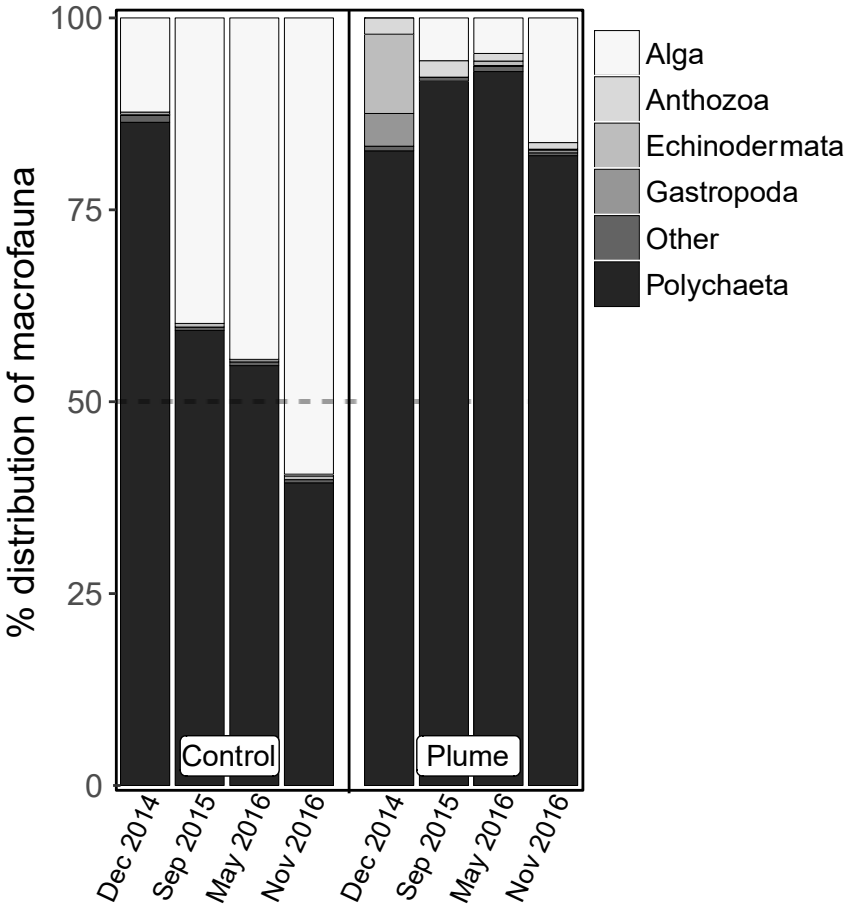

Figure S1. The percent distribution of benthic epifauna counted at the northern (control) and southern (plume) end of the beach at pre- (Dec 2014 and Sep 2015) and post-operation (May and Nov 2016).

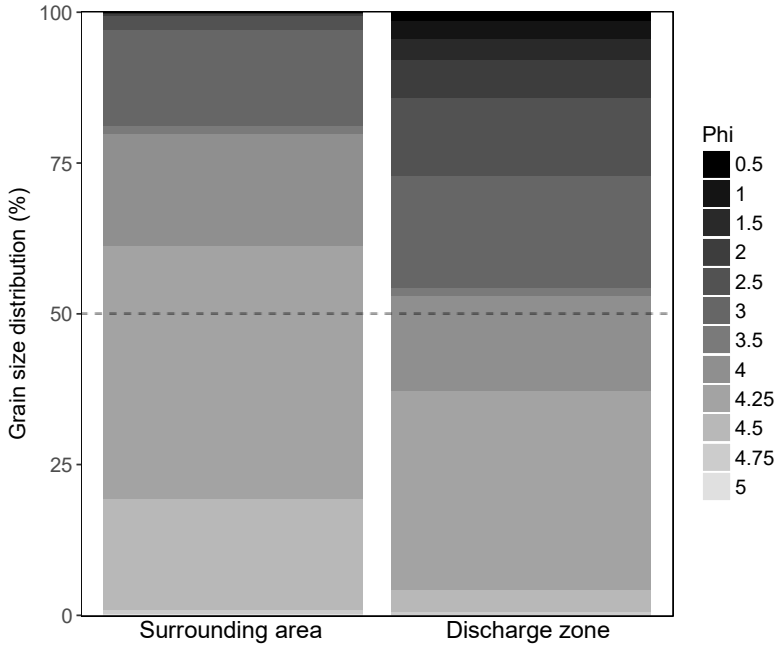

Figure 2. Grain size distribution around the discharge zone by the outfall and in the surrounding sandy area. Smaller Phi values indicate larger grains.

Table S2. Mean growth, weight and turn time (±SD) for brittle stars in control (salinity 33) and the two treatments with discharge brine after 4 weeks of incubation.

Treatment	Arm growth (mm)	Body growth (mm)	Weight (g)	Turn time (sec)
Control	0.16 (0.1)	−0.10 (0.05)	−0.01 (0.03)	5.3 (1.3)
Salinity 34	0.04 (0.09)	−0.08 (0.04)	0.006 (0.03)	4.9 (1.2)
Salinity 37	0.04 (0.2)	−0.14 (0.04)	0.02 (0.04)	7.1 (2.6)

Existing and Proposed SWRO Desalination Plants in California

Table 3. Average wave energy, orbital velocity (±SD) and areal extent of four benthic habitats within a 2 km radius around existing (*) and proposed desalination facilities in southern California and Monterey Bay.

	Plant capacity (m^3 day^{-1})	Wave Energy (J m^{-1})	Orbital Velocity	MPAs (km^2)	Eelgrass (km^2)	Surf Grass (km^2)	Kelp (Canopy) (km^2)	Hard Substrate (km^2)
Camp Pendleton	570,000	240.2 ±55.6	0.71 ±0.3	0.00	0.00	0.00	0.00	0.10
Carlsbad*	190,000	293.6 ±36.0	0.65 ±0.3	0.00	0.00	0.00	0.00	0.65
Dana Point/San Clemente	57,000	155.8 ±39.9	0.63 ±0.2	0.00	0.00	0.00	0.00	0.22
Deep Water Desalination (Moss Landing)	95,000	243.8 ±55.2	0.64 ± 0.3	0.00	0.00	0.00	0.00	0.00
Monterey Bay Aquarium*	30	55.5 ± 23.3	0.13 ±0.06	1.33	0.00	0.00	0.29	0.80
Monterey Bay Peninsula	34,000	369.2 ±120.8	0.85 ±0.4	0.00	0.00	0.00	0.00	0.00
Moss Landing	45,500	177.0 ±30.8	0.21 ±0.1	0.00	0.00	0.00	0.00	0.00
Sand City*	1,100	135.8 ±43.2	0.35 ±0.1	0.00	0.00	0.00	0.00	0.00

References

1. Erikson, H.L.; Storlazzi, C.D.; Golden, N.E. Wave Height, Peak Period, and Orbital Velocity for the California Continental Shelf. U.S. Geology Survery Data Set. 2014. Available online: http://dx.doi.org/10.5066/F7125QNQ (accessed on 26 October 2017).
2. Erikson, H.L.; Storlazzi, C.D.; Golden, N.E. Modeling Wave and Seabed Energetics on the California Continental Shelf. U.S. Geological Survey Summary of Methods to Accompany Data Release. 2014. http://dx.doi.org/10.5066/F7125QNQ (accessed on 26 October 2017).
3. Reguero, B.G.; Losada, I.J.; Méndez, F.J. A global wave power resource and its seasonal, interannual and long-term variability. *Appl. Energy* **2015**, *148*, 366–380, doi:10.1016/j.apenergy.2015.03.114.
4. Barnard, P.L.; Short, A.D.; Harley, M.D.; Splinter, K.D.; Vitousek, S.; Turner, I.L.; Allan, J.; Banno, M.; Bryan, K.R.; Doria, A.; et al. Coastal vulnerability across the Pacific dominated by El Niño/Southern Oscillation. *Nat. Geosci.* **2015**, *8*, 801, doi:10.1038/ngeo2539.